Atmospheric Research 245 (2020) 105140

Contents lists available at ScienceDirect

Atmospheric Research

journal homepage: www.elsevier.com/locate/atmosres

Dissolved organic carbon in rainwater from a karst agricultural area of Southwest China: Variations, sources, and wet deposition fluxes

Jie Zeng[a], Fu-Jun Yue[b,c,d,*], Min Xiao[e], , Zhong -Jun Wang[d], Qixin Wu[f], Cai-Qing Qin[b]

[a] Institute of Earth Sciences, China University of Geosciences (Beijing), Beijing 100083, China
[b] Institute of Surface-Earth System Science, School of Earth System Science, Tianjin University, Tianjin 300072, China
[c] Tianjin Key Laboratory of Earth Critical Zone Science and Sustainable Development in Bohai Rim, Tianjin University, Tianjin 300072, China
[d] Puding Karst Ecosystem Research Station, Institute of Geochemistry, Chinese Academy of Sciences, Anshun 562100, China
[e] Tianjin Key Laboratory of Water Resources and Environment, Tianjin Normal University, 300387 , China
[f] Key Laboratory of Karst Environment and Geohazard, Ministry of Land and Resources, Guizhou University, Guiyang 550025, China

ARTICLE INFO

Keywords:
Rainwater DOC
Source identification
Karst agricultural area
Wet deposition

ABSTRACT

Dissolved organic carbon (DOC) plays a key role among the earth-surficial ecosystem, particularly in the climate change, but very few researches focused on the rainwater DOC in karst agricultural region (vulnerable agro-ecosystem). To identify the concentrations, seasonal variations, controlling factors, deposition fluxes, and potential sources of DOC in rainwater, 85 rainwater samples were collected at the Houzhai catchment, a representative karst agriculture-intensive region in Southwest China, from June 2016 to May 2017. The concentrations and deposition flux of DOC were 0.63 mg C L^{-1} (volume-weighted mean) and 0.67 g C m^{-2} yr^{-1}. These values were lower than the Asian average value, reflecting a low level of contaminated atmospheric organic carbon in the studied area. Seasonally, low DOC concentrations were often accompanied by high deposition flux during the rainy season (heavy rainfall), suggesting that the amount of rainfall is the critical factor controlling the rainwater DOC. Moreover, long-distance migration and anthropogenic emissions were also the non-negligible impact factors. The source identification showed that both agriculture-related volatilization and fossil fuel burning (mainly coal-combustion) were the primary sources of rainwater DOC according to the correlation analysis with the major ions (typical indicators), while the contribution of other origins (e.g., plant-released, biomass burning, and windblown dust) were limited. This study clearly explores the karst-agricultural wet deposition process of DOC that would strongly benefit the study of the global carbon biogeochemical cycle.

1. Introduction

The atmosphere is a significant carbon (C) reservoir and closely related to global radiation forcing (Godoy-Silva et al., 2017). Previous studies estimated that 60% and 40% organic carbon components in atmosphere were removed in the form of wet and dry deposition and about 0.4–0.5 Gt C yr^{-1} were therefore back to the land surface via dissolved organic carbon (DOC) (Kanakidou et al., 2012; Willey et al., 2000). DOC is a widespread and vital component of atmospheric aerosols and precipitation (Xing et al., 2019).

Generally, DOC in rainwater consists of tens of thousands of carbon-containing compounds at the molecular level (Liu et al., 2020; Qi et al., 2020). These compounds are made up of various functional groups, e.g., carboxyl, carbonyl, ester, and conjugated aromatic substituents (Huang et al., 2016). Among them, the organic acids, such as formic acid, acetic acid, propionic acid, ethyl acid, malonic acid, and succinic acid, are considered as potential contributors to rainwater acidity (Zhang et al., 2011). Moreover, rainwater DOC plays a key role in the earth-surficial ecosystem, particularly in global climate change (Li et al., 2016b). For example, DOC is a powerful participant of cloud condensation nuclei due to its hygroscopic characteristics (Li et al., 2017), which causes significant effects on rainwater and climate forcing. Additionally, DOC is also a warming component in the climatic system because of it absorbs the ultraviolet light, similar to the atmospheric black carbon (Cong et al., 2015). In general, wet precipitation (rainwater) is the primary pathway for the transportation and removal of the atmospheric DOC worldwide (Iavorivska et al., 2016), which influences the atmospheric and landscape C processes. Therefore, rainwater DOC could be one of the key factors of aboveground C cycle and its deposition flux, and therefore, it is a vital input data for global C model study (Gao and Yu, 2020a; Li et al., 2016b). However, uncertainties and errors exist in the estimation of atmospheric DOC

* Corresponding author at: Institute of Surface-Earth System Science, School of Earth System Science, Tianjin University, Tianjin 300072, China
E-mail address: fujun_yue@tju.edu.cn (F.-J. Yue).

https://doi.org/10.1016/j.atmosres.2020.105140
Received 8 April 2020; Received in revised form 5 July 2020; Accepted 15 July 2020
Available online 18 July 2020
0169-8095/

deposition flux to the earth's surface, because monitoring (or routine measurement) is not continuous and systematical (Iavorivska et al., 2016), particularly the monitoring of rainwater DOC monitoring in the karst area with thin barren soil.

The spatiotemporal variations of concentrations and deposition fluxes of DOC in rainwater are quite different, which can be affected by several factors, such as DOC sources, meteorology, geography, and environmental protection policies (Iavorivska et al., 2017a). The sources of rainwater DOC are complex, which is directly derived from the solvation of atmospheric gaseous or granular organic C species (Kieber et al., 2002). These carbonaceous organic species mainly originated from the human activities (e.g., agriculture, biomass or fossil fuel burning) (Gao et al., 2020b; Iavorivska et al., 2016; Niu et al., 2019; Siudek et al., 2015; Yan et al., 2019), plant-released organic anionic species (Pantelaki et al., 2018; Zeng et al., 2019), and re-suspended dust (Xing et al., 2019). Previous studies have shown that the source contribution of rainwater DOC varies greatly in different terrestrial ecosystems. For instance, fossil fuel combustion contributes half of the rainwater DOC in urban areas (Xing et al., 2019), while biomass burning and agricultural production are considered as the major source of rainwater DOC in the agricultural regions (Godoy-Silva et al., 2017).

Although many studies focused on rainwater DOC have been carried out over the world (Iavorivska et al., 2016; Li et al., 2017; Siudek et al., 2015), including different ambient types, such as urban, rural and background regions, but very rare work was focused on the karst-related rainwater DOC, particularly in karst agro-ecosystem. Given the extreme vulnerability of karst agro-ecosystem, it is essential to obtain the information regarding to the DOC in rainwater to better understand the agro-environmental management and the C geo-chemical cycle process in this region. In order to gain additional insight into the rain-scour behavior on atmospheric DOC and the source of rainwater DOC in the Houzhai River catchment, the time series variations of the rainwater DOC concentrations in one year, were systematically investigated. The main purposes of this work are to: (1) investigate rainwater DOC concentrations, seasonal variations, and controlling factors, (2) identify the potential DOC sources, and (3) assess the DOC deposition flux in the karst region.

2. Materials and methods

2.1. Site description

The observation site was selected in the Houzhai River catchment (73.4 km^2) located in the center of the karst region, Southwest (SW) China (Hao et al., 2019). The elevation of this basin ranges from 1212 to 1552 m (Fig. 1a). The basin is characterized as a subtropical, monsoonal climate (average yearly temperature 15.1 °C) (Wang et al., 2002). Most of the rainfall events occur in May to October (80%) and result in an annual precipitation range of 1200 to 1400 mm (Chen et al., 2008). According to the variations in climate, March to May, June to August, September to November, and December to February can be defined as spring, summer, autumn, and winter. The Houzhai River catchment is widespread development of karst geomorphology (e.g., cone and cockpit). The lithology composed of Permian and Triassic age limestone and dolomite (Bai et al., 2013). The land cover of this catchment is mainly made up of agricultural land (dry land and paddy fields), buildings, forest and shrubs (Zhang et al., 2017). The cultivated land (paddy field and dry land) is generally dispersed in the mid–lower stream and accounts for 41% of the basin area (Fig. 1b), and paddy fields grow rice in the rainy season, while the dry land is used for corn growth. Moreover, the canola and vegetables are cropped during the dry season. According to the statistical data, approximately 671 and 856 t N/year of the annual nitrogenous fertilizers and organic fertilizers (manure) were used for agricultural production in Houzhai catchment (Yue et al., 2015). Among the fertilizers, di-ammonium phosphate, organic fertilizers, and urea accounted for 20–30%, 20–30%, and 40–60% (Wang et al., 2020), respectively. These fertilizers were mainly applied from April to July. The fossil fuel combustion in the catchment occurs mainly in winter, including the dwellings' heating requirements and coal-fired power plants. Based on the perspective of catchment hydrology, one site (HZV, 105°41′15″E, 26°16′09″N, 1220 m asl.) was selected to collect rainwater samples (Fig. 1a). This site located in the flat plains, downstream of the catchment, within a mixed usage profile of buildings (Houzhai village) and agricultural land (paddy field and dry land), which represents a significant human influence.

2.2. Sample collection and measurement

Rainwater samples collection was performed by a 65 cm diameter polyethylene (PE) sampler installed on a building-rooftop approximately 8 m above the ground. The potential dust deposition on the non-rainy days was avoided via a PE lid. Before sampling, the samplers were cleaned with deionized-water, air-dried, lidded, and then prepared for the next sampling. The sampling was performed on a daily basis during the rainy days. Ultimately, 80 rainwater samples were collected from June 2016 to May 2017, and most of them were obtained during the rainy season.

Here, the samples were used for DOC concentration measurement, after being filtered via 0.45 μm membrane filters (Millipore). The DOC concentrations of rainwater were determined in the form of CO_2 by the

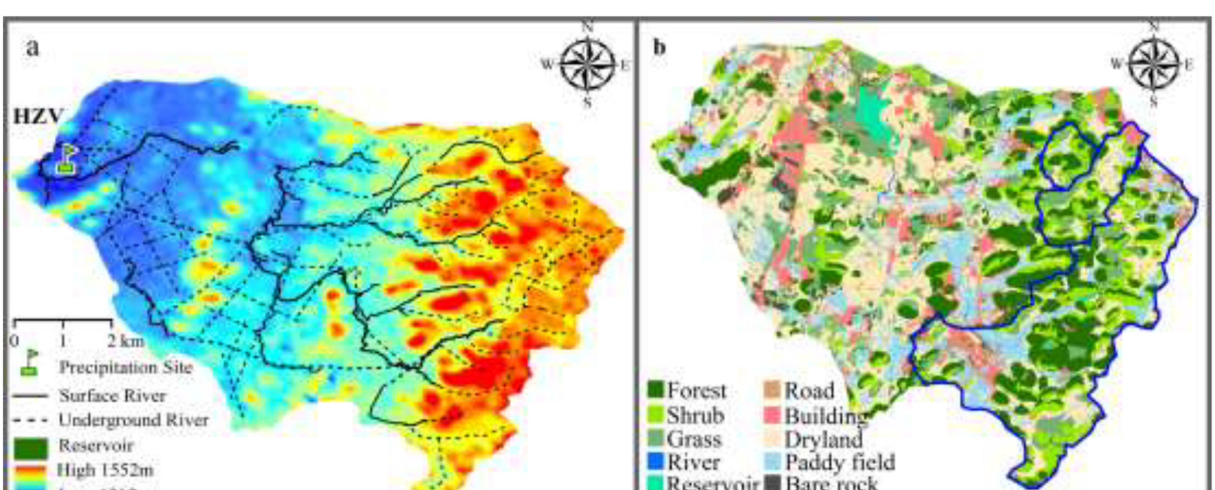

Fig. 1. Map of study catchment (a) topography and observation site; (b) land use/cover. Map modified from (Yue et al., 2019).

sodium persulfate oxidation method (TOC analyzer, Aurora 1030, OI Analytical, USA) (Li et al., 2010; Qin et al., 2019). All the laboratory work was conducted at the Institute of Geochemistry, Chinese Academy of Sciences. For the method validation, the procedural blank was measured together with the standards, samples, and the repeated samples, by applying the same protocol. The analytical precision is better than 5%. The major ions concentrations used in this study were reported in previous work (Zeng et al., 2020c).

2.3. Calculations

The volume-weighted mean (VWM) DOC concentrations of rainwater samples were calculated using the follow equations (Qin et al., 2016):

$$C = \frac{\sum C_i P_i}{\sum P_i} \tag{1}$$

where C represents the VWM concentration of DOC, C_i is the DOC concentration of each sample (mg L^{-1}), P_i is the precipitation amount of the corresponding sample. The precipitation amount data were taken from our previous study in Houzhai catchment (Yue et al., 2019).

The monthly DOC deposition flux was estimated as follows (Meng et al., 2019):

$$WD = 0.001 \times C_{VWM} \times P_{month} \tag{2}$$

where WD (g C m^{-2}) is the monthly DOC deposition flux, C_{VWM} represents the monthly VWM DOC concentration of rainwater (mg L^{-1}), R_i is the monthly rainfall amount (mm). The sum of the monthly DOC fluxes (June 2016 to May 2017) is defined as annual wet deposition flux.

2.4. Data processing method

For the statistical analyses of obtained data, the normal distribution of DOC data was calculated via the Kolmogorov–Smirnov (K–S) test, one of the non-parametric tests commonly applied to analysis sample data set. According to the results of the normal distribution test (non-normally distribution), Spearman's rank correlation coefficient and principal component analysis (PCA) were applied to reflect the relationship between DOC concentrations and other ion concentrations. All the data processing was performed using SPSS 21.0 (IBM, Armonk, NY, USA).

3. Results and discussion

3.1. DOC of karst-agricultural rainwater

3.1.1. Concentrations comparison

The DOC concentrations of rainwater collected from the Houzhai catchment were summarized in Table S1 and plotted in Fig. 2. It is obvious that the mean concentration (1.46 mg C L^{-1}) was greater than the VWM concentration (0.63 mg C L^{-1}), suggesting high concentration generally tended to happen with low amounts of rainfall, which is consistent with the data observed around the world (Fig. 2). The concentrations of rainwater DOC in the Houzhai catchment were highly variable across the studied period, the highest DOC concentration (8.18 mg C L^{-1}) was almost 73 times higher than the lowest DOC concentration (0.11 mg C L^{-1}). The highest DOC concentration occurred on 14th May 2017 (low rainfall = 1.6 mm), whereas the lowest DOC concentration accompanied by a large daily rainfall amount (32.8 mm) on 4th August 2016, implying a significant influence from the rainfall. Accordingly, the rainwater DOC in this study is 1.2 to 91 times of the low background value in the remote area (0.09 mg C L^{-1}, Everest) (Li et al., 2016a), with an average of 16 times higher than the low background value, indicating the obvious DOC external input. K–S test showed that the DOC contents were non-normally distributed ($p < .1$) in the sampling period. Combining the K–S test result and standard deviation (SD, 1.48 mg C L^{-1}), the mean DOC concentration of rainwater has been significantly affected by the tremendously high values. Therefore, the VWM concentration rather than mean concentration of DOC is more suitable for comparison, which is also widely applied in the environmental researches (Iavorivska et al., 2016; Li et al., 2017; Pantelaki et al., 2018).

Globally, the VWM concentration of rainwater DOC (0.63 mg C L^{-1}) in this study is only approximately a quarter of the Asian average level (2.65 mg C L^{-1}) or global average level (2.64 mg C L^{-1}) (Iavorivska et al., 2016) (Fig. 2), even close to the various background sites (0.02–0.86 mg C L^{-1}), such as the Himalayas, Tibet and the Azores of Portugal (Cerqueira et al., 2010; Li et al., 2017; Li et al., 2016b). In the agriculture-dominated areas, the present VWM (or mean) DOC concentration is comparable to that found in Pennsylvania, USA and South Island, New Zealand (Iavorivska et al., 2017b; Kieber et al., 2002). In contrast, the rainwater DOC concentration in the urban area (e.g., Northern China, Seoul Korea) is about two to six times higher than that in present study (Fig. 2), particularly in areas of relatively heavily air-polluted areas caused by large quantities of pollutant discharge, such as Northern China and Beijing (Pan et al., 2010). Moreover, compared to most of the coastal regions (Fig. 2), which are highly susceptible to atmospheric oceanic currents, the rainwater DOC concentration in present study (inland monsoon region) is much lower. The results discussed above suggested that the contribution of exogenous organic carbon input is relatively low in terms of the DOC concentration of rainwater in the Houzhai catchment.

3.1.2. Seasonal variation and affecting factors

In the study period, a total of 1064 mm (close to the annual mean rainfall amount) of rainfall was trapped and collected, and the monthly rainfall amount varied significantly from 6.0 mm (December) to 387.5 mm (June). Accordingly, the monthly VWM DOC concentrations were calculated based on Eq. (1) and plotted in Fig. 3. The monthly rainwater DOC concentrations fluctuated between 0.4 and 4.0 mg C L^{-1} (September and December, Fig. 3). The monthly DOC VWM concentration displayed an almost completely opposite variation trend to the rainfall amount. This indicated that the rainfall amount is the critical influencing factor for the rainwater DOC, a finding which in accord with another study (Li et al., 2016b).

To further illuminate the opposite trend between DOC concentration and rainfall amount, the relationship between rainfall and DOC concentration was plotted in Fig. 4a. An opposite relationship was observed between DOC concentration and rainfall amount (Fig. 4a). The Spearman's rank correlation coefficient between DOC concentration and rainfall data after logarithmic processing revealed that DOC concentrations in the Houzhai catchment were mostly influenced by the dilution effect of high precipitation ($r = -0.57$, $p < .01$) (Fig. 4b), which is widely supported by the previous studies (Li et al., 2016b; Yan and Kim, 2012). In that dilution effect, the atmospheric C species could be efficiently scoured (mainly the below-cloud scouring processes) via the initial rain-stage, leading to the high DOC content occurred with small rainfall. Conversely, without the persistent supplies of suspended carbonaceous materials, the DOC content of the subsequent continuous rain-stage inclines to be reduced gradually and remained at a low concentration (Fig. 4a, the gray background box). The critical value of the initial rainfall amount is approximately 10 mm from Fig. 4a, which suggested that the atmospheric carbonaceous aerosols were basically scoured completely at this rainfall amount condition. However, the DOC concentrations of rainwater were closer to those of cloud-water (carbonaceous aerosols dissolved in cloud droplets) when the rainfall amount exceeds 10 mm, mainly reflecting the within-cloud process (Xing et al., 2019; Zeng et al., 2020a). In this case (rainfall amount > 10 mm), the dilution effect of DOC was very weak, the long-distance migration is therefore another non-negligible impacting factor for rainwater DOC (Godoy-Silva et al., 2017).

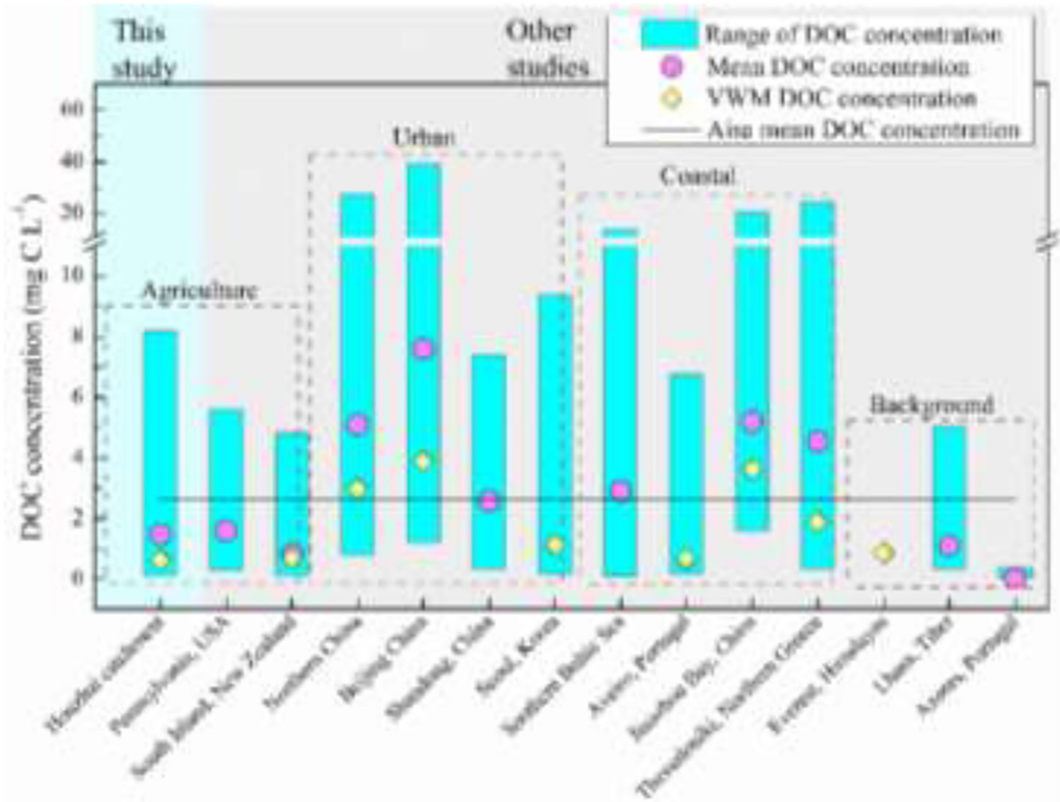

Fig. 2. Rainwater DOC concentrations in Houzhai catchment and other regions around the world. Data sources: (Cerqueira et al., 2010; Iavorivska et al., 2016; Iavorivska et al., 2017b; Kieber et al., 2002; Li et al., 2017; Li et al., 2016b; Pan et al., 2010; Pantelaki et al., 2018; Santos et al., 2013; Wang et al., 2016b; Witkowska and Lewandowska, 2016; Xing et al., 2019; Yan and Kim, 2012).

It is noteworthy that the VWM DOC concentrations from December to March varied remarkably while the rainfall amount trend smooth in these months (Fig. 3). This may also suggest that the content of gaseous soluble organic matter and suspended organic C particles in the atmosphere can impact the rainwater DOC concentration as well (Herckes et al., 2002; Wei et al., 2020; Wei et al., 2019b). The research from the USA also confirmed that the short-term regional high-intensity emissions and atmospheric photo-chemical conversions might accelerate the increase of rainwater DOC concentrations of some rainfall events (Iavorivska et al., 2017b). Moreover, our previous study have confirmed that more anthropogenic emissions would be accumulated in the atmosphere with increased human activities in winter (December to

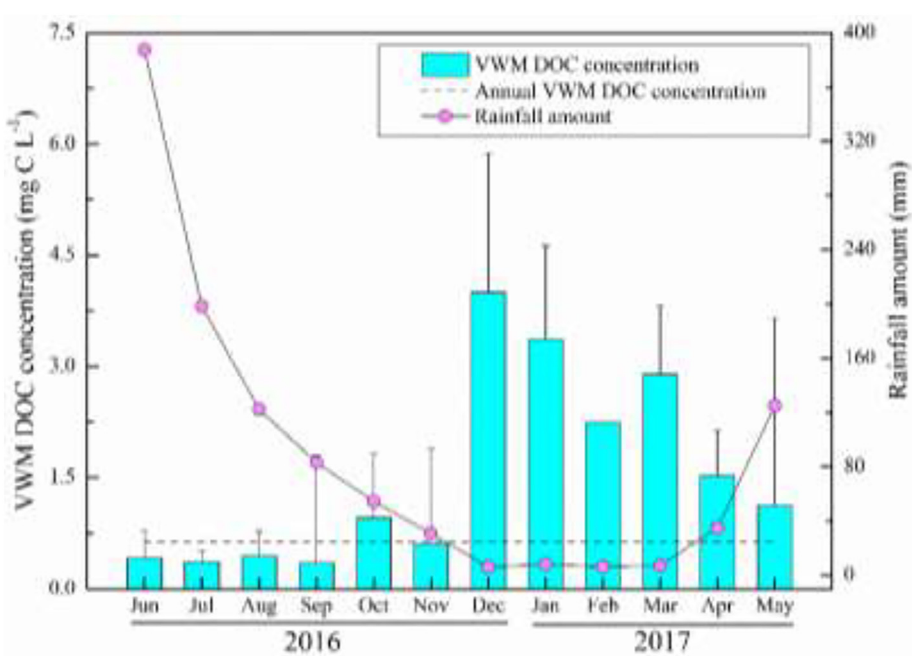

Fig. 3. Monthly variations of VWM DOC concentrations of rainwater in Houzhai catchment.

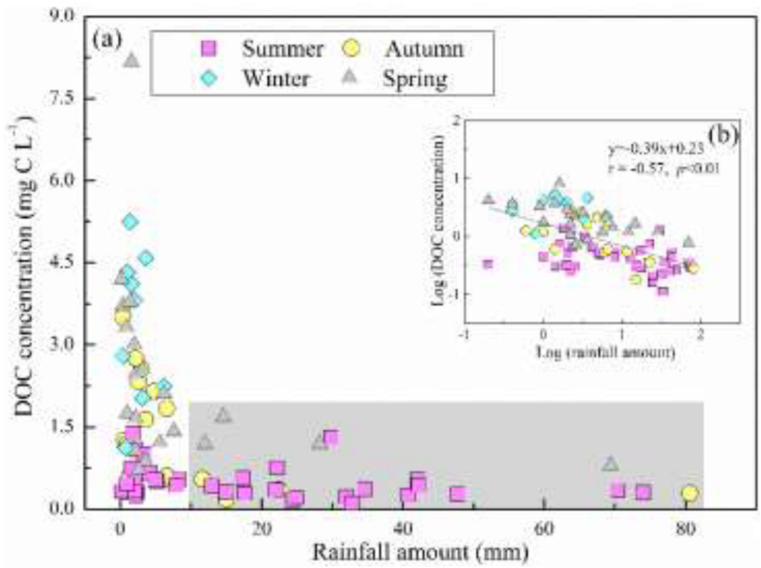

Fig. 4. Correlations between DOC concentration and precipitation in Houzhai catchment from 2016-Summer to 2017-Spring. (a) raw data of DOC concentration v.s precipitation; (b) logarithmic DOC content v.s logarithmic precipitation.

February), such as heating of dwellings (coal combustion) (Zeng et al., 2020b), which would subsequently result in higher levels of gaseous soluble organic species and particulate organic C in the air. Therefore, the seasonal source variations e.g., anthropogenic emissions, could be responsible for influencing the rainwater DOC concentration, as shown in Fig. 3, which is also supported by the other study (Szidat et al., 2006).

3.2. Origins of DOC

3.2.1. Correlation analysis and principal component analysis

Rainwater DOC has multifaceted sources including natural and human-derived origins. The transportation distance of some initial atmospheric OC (mainly in the form of carbonaceous aerosols from natural/anthropogenic sources) is up to thousands of kilometers after emission, and can even migrate to the polar regions and be deposited there (Cao et al., 2009; Yan et al., 2019). On the other side, the migration distance of some local OC (e.g., low molecular weight organic acids) is relatively short, and can be quickly captured by rainwater and deposited (Zhang et al., 2011). Correlation analysis is one of the most commonly applied methods for exploring the main origins of atmospheric materials (Han et al., 2019; Keresztesi et al., 2020). In this study, some typical signature chemical components (comprising Ca^{2+}, NH_4^+, Na^+, Mg^{2+}, K^+, SO_4^{2-}, NO_3^-, Cl^-, and F^-) in rainwater were applied in the correlation analysis for qualitatively recognizing the DOC origins. As shown in Fig. 5, both the correlation and principal component analysis (PCA) showed that DOC origins were significantly different from the typical sea source (SS) Na^+ (without significant correlation, plotted in the different PC, Fig. 5a and b). Therefore, given the fact that our study area is far from the ocean, the SS-DOC was negligible. The correlation coefficients between the rainwater DOC and the non-sea source (NSS) part of the major ions were therefore performed to distinguish the DOC sources (Fig. 6).

3.2.2. Potential source identification

Generally, the agriculture-associated NH_3 volatilization from fertilizer (e.g., urea) and human/animal excrement applied in agricultural soils is the primary sources of atmospheric NH_4^+ (Lee et al., 2012; Xiao et al., 2012). The strong correlation between rainwater DOC and NH_4^+ (Fig. 6a) suggests that agriculture-related organics volatilization from nitrogenous/organic fertilizers (urea and manure) are important sources of rainwater DOC at the Houzhai catchment. Moreover, the NH_4^+/NO_3^- molar ratio can be an effective value to identify the agricultural and non-agricultural sources, and the NH_4^+/NO_3^- ratio generally exceed 1 in the agriculture-dominated areas (Lee et al., 2012; Wang and Han, 2011; Zhang et al., 2008), while the $NH_4^+/NO_3^- < 1.0$ is mainly observed in some highly urbanized and industrialized regions, showing the characteristics of NO_3^- dominant nitrogen composition, such as Central New York (Fahey et al., 1999). In diagram of DOC vs NH_4^+/NO_3^- of this study, most of the samples were scattered on the right side of the line of $NH_4^+/NO_3^- = 1$ (Fig. 7a). This further supports the significant contribution of agricultural production to the rainwater DOC.

Rainwater has been confirmed as an important sink of OC derived from fossil fuel combustion (e.g., coal and gasoline) in the atmosphere. In the Houzhai catchment, significant positive correlations among rainwater DOC and NO_3^- and NSS-SO_4^{2-}, were observed (Figs. 6b and c), the two typical products of fossil fuel combustion (NO_x and SO_x, and their ramification NO_3^- and NSS-SO_4^{2-}) (Charlson and Rodhe, 1982; Wei et al., 2019a; Willey et al., 2006), which implied that rainwater DOC might have origins of fossil fuel combustion similar to NO_x and SO_x. Typically, these fossil fuel sources are usually divided into fixed emission sources (coal combustion in industry, power plants and house heating) and mobile sources (vehicle gasoline combustion) (Chandra et al., 2005; Han et al., 2010). There was only one sample that presents a SO_4^{2-}/NO_3^- ratio of less than 1 in the diagram of DOC vs SO_4^{2-}/NO_3^- of this study (Fig. 7b), which indicated that the contributions of fixed emission sources were much higher than those of mobile sources to the rainwater DOC (Arimoto et al., 1996; Han et al., 2010; Xing et al., 2019). This can be further supported by the existence of coal-fired power plants, heating requirements in winter (relatively higher SO_4^{2-}/NO_3^- ratio than other seasons, cyan diamond in Fig. 7b) and relatively few vehicles in the Houzhai catchment. Therefore, we concluded that fossil fuel burning (mainly coal-combustion) is another important source of rainwater DOC at Houzhai catchment.

NSS-K^+ was generally regarded as a tracer for biomass burning (Godoy-Silva et al., 2017). Many studies have shown that biomass burning contributes significantly to global atmospheric DOC, particularly in areas with extensive agricultural production. This is also confirmed via the correlation between NSS-K^+ and DOC in present study (Fig. 6d). However, given that the specific farming practices from biomass burning mainly occurred after the harvest, that is, biomass

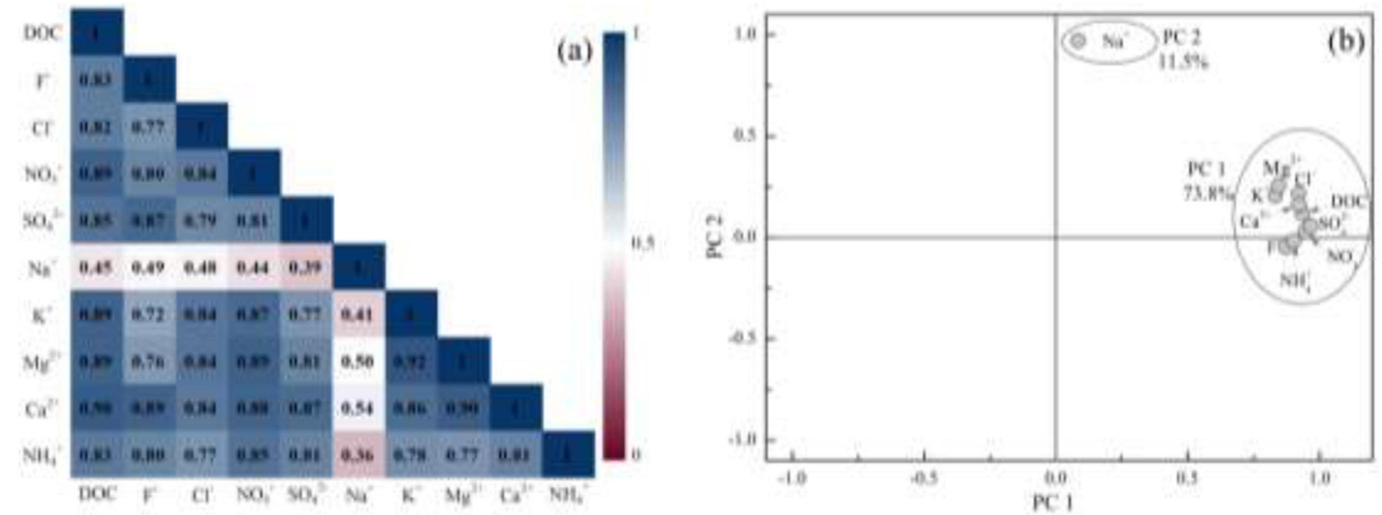

Fig. 5. The correlation analysis (a) and principal component analysis (b) of rainwater and major ions in Houzhai catchment. The Spearman's rank correlation coefficient was applied for the DOC concentrations due to the data were not normally distributed, the significance level is $p < .05$.

burning activities only lasted for about one month per year, and therefore, the contribution of biomass burning to rainwater DOC is very limited. In contrast, the plant-released organic anionic species (e.g. oxalate) in this agricultural catchment can be considered as a potential source of rainwater DOC, which can be supported by the slight imbalance between cations and anions in rainwater (implying the existence of the organic anions in rainwater) (Wu et al., 2012). Moreover, the atmospheric windblown dust (Ca and Mg enriched materials) (Hoffman et al., 1977; Rao et al., 2017) can also be a noteworthy source of rainwater DOC in the Houzhai catchment according to the result presented in Figs. 6e and f.

3.3. Wet deposition flux of DOC

According to the monthly rainfall amount and monthly VWM concentrations of rainwater DOC in Houzhai catchment, the monthly wet deposition flux of DOC was estimated using Eq. (2). Differing from the monthly VWM DOC concentration, a significant parallel variation was observed between the deposition flux and the precipitation (Fig. S1), which observed the largest monthly DOC deposition fluxes in June (Summer) and the smallest in February (Winter) with a range of 13.9–159.9 mg C m^{-2} $month^{-1}$ (Fig. S1). This is in line with other studies (Li et al., 2016b; Xing et al., 2019). It is noteworthy that the rainfall amount in May was only one third of that in June, while the wet DOC deposition flux in May was little different from that in June (Fig. S1). This could be explained by the fact that May is the month with the most intense agricultural fertilization and fastest crop growth (Wang et al., 2016a), which causes the more agriculture-derived organic matters input to the atmosphere, which can be further trapped by the rainwater.

Overall, the annual wet DOC deposition flux was approximately 0.67 g C m^{-2} yr^{-1} in the Houzhai catchment (Fig. 8 and Table S1), from which the wet DOC deposition fluxes in May and June account for almost half of the annual wet DOC deposition flux (45%, Fig. S1). In Fig. 8, our wet DOC deposition flux is well below the global average (3.4 g C m^{-2} yr^{-1}), while it is close to background sites (0.16 to 0.63C m^{-2} yr^{-1} in Everest and Lhasa, Himalayas) and a coastal island with little human disturbance (0.4C m^{-2} yr^{-1} in the Azores, Portugal) (Cerqueira et al., 2010; Iavorivska et al., 2016; Li et al., 2017; Li et al., 2016b). Unsurprisingly, the annual wet DOC deposition flux in Houzhai catchment was also lower than other agricultural and urban regions (1.8 to 7.3C m^{-2} yr^{-1}) (Godoy-Silva et al., 2017; Pan et al., 2010; Pantelaki et al., 2018; Wang et al., 2016b; Witkowska and Lewandowska, 2016; Xing et al., 2019; Yan and Kim, 2012), reflecting a low contamination level of atmospheric organic carbon in the studied karst agricultural catchment.

According to the area of Houzhai catchment (73.4 km^2) and the annual wet DOC deposition rate (0.67 g C m^{-2} yr^{-1}), the wet DOC deposition loading into catchment was calculated to be 49.2 t C yr^{-1}. The annual runoff of Houzhai catchment is about 32 × 10^6 m^3 yr^{-1} (Yue et al., 2019; Zhang et al., 2020), and fluvial DOC flux by Houzhai River is completely controlled by the runoff. Therefore, the fluvial DOC flux occurs via the total outlet (~200 m from HZV) could represent the total DOC flux of the catchment. Combined with the fluvial DOC concentrations (0.81–1.10 mg L^{-1}) of total outlet (Qin et al., 2019) and the annual runoff, the annual fluvial DOC loading of Houzhai catchment is roughly evaluated to be 25.9–35.2 t C yr^{-1}. It can be obviously seen than the wet DOC deposition loading is about 1.6 times of the fluvial DOC loading, which highlights the potential significant influence of the wet DOC deposition on surface drainage of Houzhai catchment.

4. Conclusions

In conclusion, we investigated the one-year data on the rainwater DOC to identify the concentrations, seasonal variations, controlling factors, deposition flux, and potential sources in a karst area with a vulnerable agro-ecosystem (the Houzhai catchment), SW China. The results revealed that Houzhai catchment has undergone slight contamination of atmospheric organic matter based on the low concentration (0.63 mg C L^{-1}) and wet deposition flux (0.67 g C m^{-2} yr^{-1}) of rainwater DOC. The seasonal variations of DOC concentration and deposition flux indicated that the precipitation is the critical reason influencing the rainwater DOC. In addition, long-distance migration and anthropogenic emissions were also potential impacting factors. Moreover, the agriculture-related volatilization (e.g., nitrogenous fertilizer and organic fertilizers) and fossil fuel burning (primarily coal-combustion) were considered as the primary origins of rainwater DOC in terms of the correlation analysis with rainwater chemicals (and their molar ratio), while the contribution of biomass burning, plant-released, and windblown dust to the rainwater DOC were negligible. This work complements the rainwater DOC study in karst agricultural areas and contributed to the corpus of knowledge on the global carbon biogeochemical cycle.

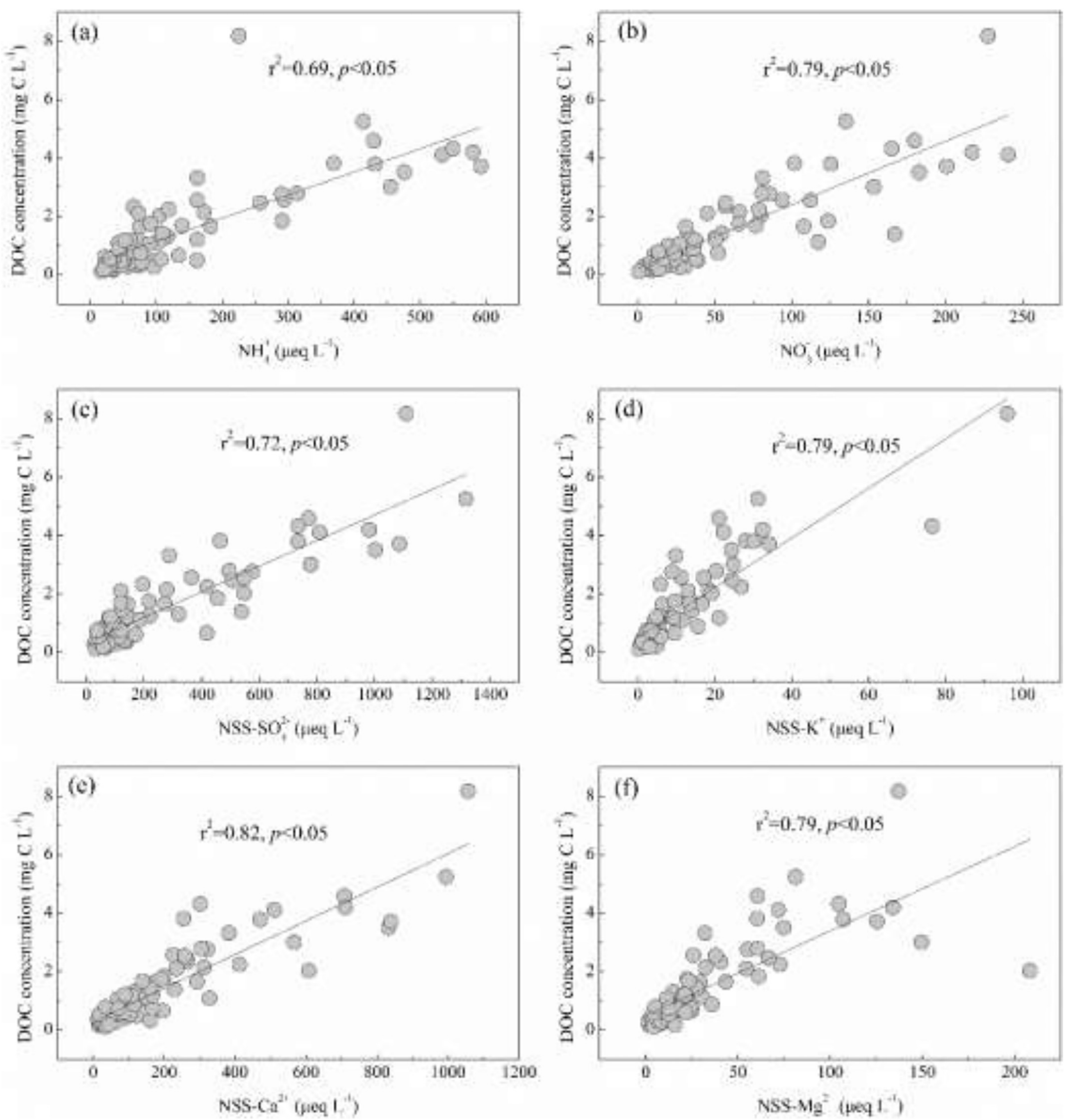

Fig. 6. Correlations between DOC concentrations and typical chemical components (Spearman's rank correlation coefficient, see more details in section 2.4): (a) NH_4^+, (b) NO_3^-, (c) NSS-SO_4^{2-}, (d) NSS-K^+, (e) NSS-Ca^{2+}, (f) NSS-Mg^{2+}. The non-sea salt (NSS) part of major ions were used to avoid the potential effects of the sea salt sources, while the NH_4^+ and NO_3^- were almost all from NSS sources and therefore can represent the NSS-NH_4^+ and NSS-NO_3^- (Xing et al., 2019; Zeng et al., 2020c).

Declaration of Competing Interest

The authors declare that they have no known competing financial interests or personal relationships that could have appeared to influence the work reported in this paper.

Acknowledgments

This research was funded by the Strategic Priority Research Program of Chinese Academy of Sciences, Grant No. XDB40000000; National Natural Science Foundation of China [grant number 41571130072]; Independent Innovative Foundation of Tianjin University [grant number 2020XY-0025]; the Fundamental Research Funds for the Central Universities [grant number 2652019247].

Credit author statement

Jie Zeng: Investigation, Data curation, Formal analysis, Writing -

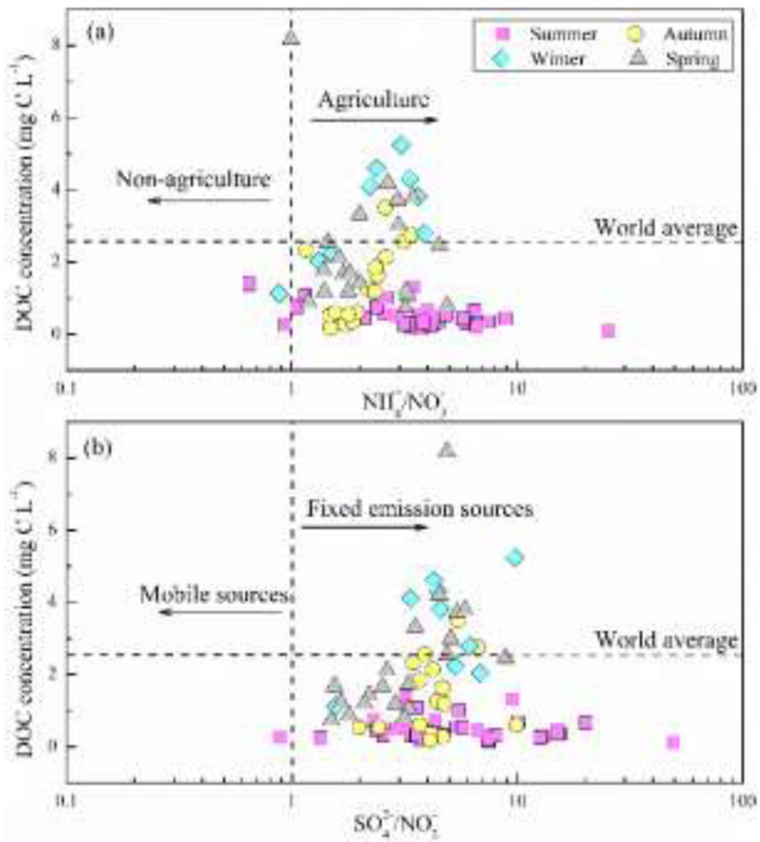

Fig. 7. The covariations of rainwater DOC concentrations with (a) NH_4^+/NO_3^- and (b) SO_4^{2-}/NO_3^- ratio (equivalent ratio) in Houzhai catchment. The imaginary lines (reference values) are from (Arimoto et al., 1996; Lee et al., 2012; Xiao et al., 2013).

original draft. **Fu-Jun Yue:** Conceptualization, Supervision, Writing - review & editing. **Min Xiao:** Review & editing. **Zhong-Jun Wang:** Formal analysis, Methodology, Investigation, Review & editing **Qixin Wu:** Data curation, Review & editing. **Caiqing Qin:** Data curation, Investigation, Review & editing.

Appendix A. Supplementary data

Supplementary data to this article can be found online at https://doi.org/10.1016/j.atmosres.2020.105140.

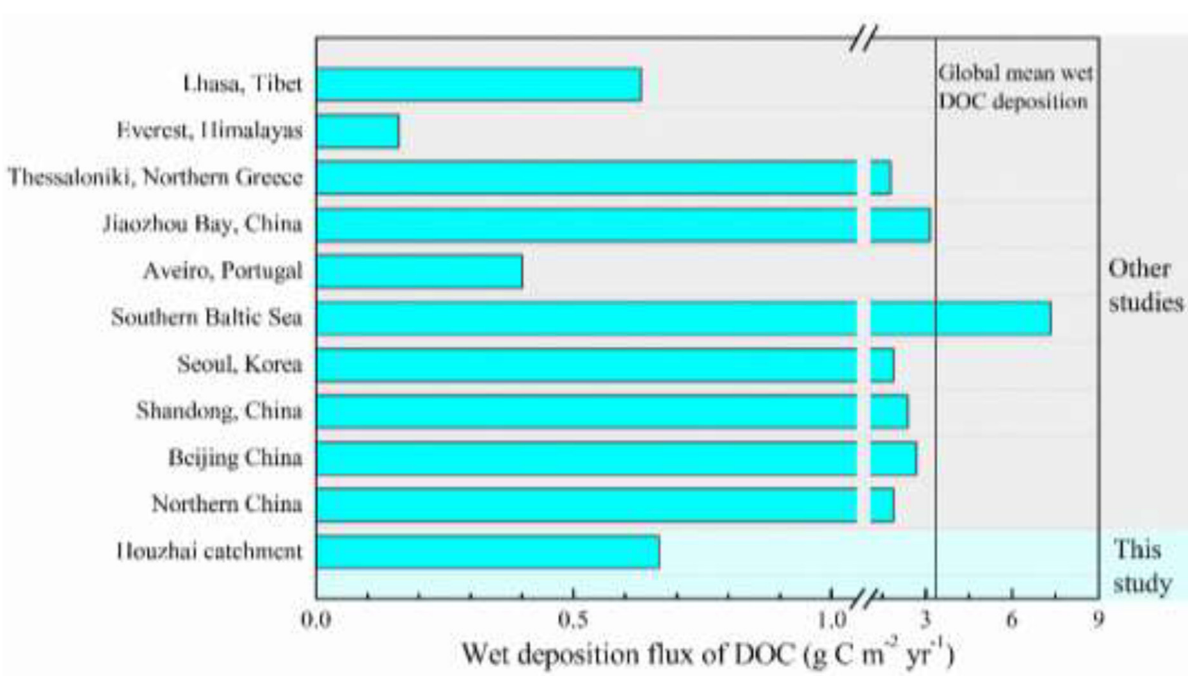

Fig. 8. Wet deposition fluxes of DOC in Houzhai catchment, other observed results around the world are also presented. Data sources are same to Fig. 2.

References

Arimoto, R., et al., 1996. Relationships among aerosol constituents from Asia and the North Pacific during PEM-West a. J. Geophys. Res.-Atmos. 101, 2011–2024.

Bai, X., Zhang, X., Long, Y., Liu, X., Siyu, Z., 2013. Use of ^{137}Cs and $^{210}Pb_{ex}$ measurements on deposits in a karst depression to study the erosional response of a small karst catchment in Southwest China to land-use change. Hydrol. Process. 27, 822–829.

Cao, J.-J., et al., 2009. Concentrations, seasonal variations, and transport of carbonaceous aerosols at a remote Mountainous region in western China. Atmos. Environ. 43, 4444–4452.

Cerqueira, M., et al., 2010. Particulate carbon in precipitation at European background sites. J. Aerosol Sci. 41, 51–61.

Chandra, M.P., Venkata, M.S., Reddy, S.J., 2005. Rainwater chemistry at a regional representative urban site: influence of terrestrial sources on ionic composition. Atmos. Environ. 39, 999–1008.

Charlson, R.J., Rodhe, H., 1982. Factors controlling the acidity of natural rainwater. Nature 295, 683–685.

Chen, X., Chen, C., Hao, Q., Zhang, Z., Shi, P., 2008. Simulation of rainfall-underground outflow responses of a karstic watershed in Southwest China with an artificial neural network. Water Sci. and Eng. 1, 1–9.

Cong, Z., et al., 2015. Carbonaceous aerosols on the south edge of the Tibetan Plateau: concentrations, seasonality and sources. Atmos. Chem. Phys. 15, 1573–1584.

Fahey, T.J., et al., 1999. Nitrogen Deposition in and around an Intensive Agricultural District in Central New York. J. Environ. Qual. 28, 1585–1600.

Gao, Y., Yu, G., 2020a. Regional coupled C-N-H_2O cycle processes and associated driving mechanisms. Sci. China Earth Sci. 1–10.

Gao, Y., et al., 2020b. Human activities aggravate nitrogen deposition pollution to inland water over China. Natl. Sci. Rev. 7, 430–440.

Godoy-Silva, D., Nogueira, R.F.P., Campos, M.L.A.M., 2017. A 13-year study of dissolved organic carbon in rainwater of an agro-industrial region of São Paulo state (Brazil) heavily impacted by biomass burning. Sci. Total Environ. 609, 476–483.

Han, G., Tang, Y., Wu, Q., Tan, Q., 2010. Chemical and strontium isotope characterization of rainwater in karst virgin forest, Southwest China. Atmos. Environ. 44, 174–181.

Han, G., Song, Z., Tang, Y., Wu, Q., Wang, Z., 2019. Ca and Sr isotope compositions of rainwater from Guiyang city, Southwest China: Implication for the sources of atmospheric aerosols and their seasonal variations. Atmos. Environ. 214, 116854.

Hao, Z., Gao, Y., Sun, X., Wen, X., Xiong, B., 2019. Determining nitrogen and carbon footprints to reveal regional gross primary productivity and differentiation characteristics in karst and non-karst watersheds, China. J. Clean. Prod. 227, 1149–1160.

Herckes, P., et al., 2002. Organic Matter in Central California Radiation Fogs. Environ. Sci. Technol. 36, 4777–4782.

Hoffman, E.J., Huffman, G.L., Fletcher, I.S., Duce, R.A., 1977. Further consideration of alkali and alkaline earth geochemistry of marine aerosols: results of a study of marine aerosols collected on Bermuda. Atmos. Environ. 11, 373–377.

Huang, H., Chow, C.W.K., Jin, B., 2016. Characterisation of dissolved organic matter in stormwater using high-performance size exclusion chromatography. J. Environ. Sci. 42, 236–245.

Iavorivska, L., Boyer, E.W., DeWalle, D.R., 2016. Atmospheric deposition of organic carbon via precipitation. Atmos. Environ. 146, 153–163.

Iavorivska, L., Boyer, E.W., Grimm, J.W., 2017a. Wet atmospheric deposition of organic carbon: an underreported source of carbon to watersheds in the northeastern United States. J. Geophys. Res.-Atmos. 122, 3104–3115.

Iavorivska, L., et al., 2017b. Variability of dissolved organic carbon in precipitation during storms at the Shale Hills critical Zone Observatory. Hydrol. Process. 31, 2935–2950.

Kanakidou, M., et al., 2012. Atmospheric fluxes of organic N and P to the global ocean. Glob. Biogeochem. Cycles 26.

Keresztesi, Á., et al., 2020. Assessing the variations in the chemical composition of rainwater and air masses using the zonal and meridional index. Atmos. Res. 237, 104846.

Kieber, R.J., Peake, B., Willey, J.D., Avery, G.B., 2002. Dissolved organic carbon and organic acids in coastal New Zealand rainwater. Atmos. Environ. 36, 3557–3563.

Lee, K.-S., et al., 2012. Nitrogen isotope ratios of dissolved organic nitrogen in wet precipitation in a metropolis surrounded by agricultural areas in southern Korea. Agric. Ecosyst. Environ. 159, 161–169.

Li, C., et al., 2016a. Carbonaceous matter deposition in the high glacial regions of the Tibetan Plateau. Atmos. Environ. 141, 203–208.

Li, C., et al., 2016b. Concentration, sources, and flux of dissolved organic carbon of precipitation at Lhasa city, the Tibetan Plateau. Environ. Sci. Pollut. Res. 23, 12915–12921.

Li, C., et al., 2017. Deposition and light absorption characteristics of precipitation dissolved organic carbon (DOC) at three remote stations in the Himalayas and Tibetan Plateau, China. Sci. Total Environ. 605-606, 1039–1046.

Li, S.-L., et al., 2010. Geochemistry of dissolved inorganic carbon and carbonate weathering in a small typical karstic catchment of Southwest China: Isotopic and chemical constraints. Chem. Geol. 277, 301–309.

Liu, M., Han, G., Zhang, Q., 2020. Effects of agricultural abandonment on soil aggregation, soil organic carbon storage and stabilization: results from observation in a small karst catchment, Southwest China. Agric. Ecosyst. Environ. 288, 106719.

Meng, Y., et al., 2019. Characterization of inorganic ions in rainwater in the megacity of Shanghai: Spatiotemporal variations and source apportionment. Atmos. Res. 222, 12–24.

Niu, H., et al., 2019. Dissolved organic carbon in summer precipitation and its wet deposition flux in the Mt. Yulong region, southeastern Tibetan Plateau. J. Atmos. Chem. 76, 1–20.

Pan, Y., et al., 2010. Study on dissolved organic carbon in precipitation in Northern China. Atmos. Environ. 44, 2350–2357.

Pantelaki, I., Papatzelou, A., Balla, D., Papageorgiou, A., Voutsa, D., 2018. Characterization of dissolved organic carbon in rainwater of an urban/coastal site in Mediterranean area. Sci. Total Environ. 627, 1433–1441.

Qi, Y., Fu, P., Volmer, D.A., 2020. Analysis of natural organic matter via fourier transform ion cyclotron resonance mass spectrometry: an overview of recent non-petroleum applications. Mass Spectrom. Rev. https://doi.org/10.1002/mas.21634.

Qin, C., Wang, Y., Peng, Y., Wang, D., 2016. Four-year record of mercury wet deposition in one typical industrial city in Southwest China. Atmos. Environ. 142, 442–451.

Qin, C., Li, S.-L., Yue, F.-J., Xu, S., Ding, H., 2019. Spatiotemporal variations of dissolved inorganic carbon and controlling factors in a small karstic catchment, Southwestern China. Earth Surf. Process. Landf. 44, 2423–2436.

Rao, W., et al., 2017. Chemical and Sr isotopic characteristics of rainwater on the Alxa Desert Plateau, North China: Implication for air quality and ion sources. Atmos. Res. 193, 163–172.

Santos, P.S.M., Santos, E.B.H., Duarte, A.C., 2013. Seasonal and air mass trajectory effects on dissolved organic matter of bulk deposition at a coastal town in South-Western Europe. Environ. Sci. Pollut. Res. 20, 227–237.

Siudek, P., Frankowski, M., Siepak, J., 2015. Seasonal variations of dissolved organic carbon in precipitation over urban and forest sites in Central Poland. Environ. Sci. Pollut. Res. 22, 11087–11096.

Szidat, S., et al., 2006. Contributions of fossil fuel, biomass-burning, and biogenic emissions to carbonaceous aerosols in Zurich as traced by C-14. J. Geophys. Res.-Atmos. 111.

Wang, H., Han, G., 2011. Chemical composition of rainwater and anthropogenic influences in Chengdu, Southwest China. Atmos. Res. 99, 190–196.

Wang, L., Zeng, C., Meng, H., Chang, W., 2016a. Water geochemistry and dissolution rates of the karst-dominated Houzhai River basin, China. Toxicol. Environ. Chem. 98, 648–657.

Wang, L.-c., Zhang, J.-x., Zhou, Y.-k., Chen, X.-l., Du, J.-k., 2002. Approach of deterministic geomorphologic instrantaneous unit hydrograph to hydrological processes' simulation in Karst area. Chin. Geogr. Sci. 12, 354–358.

Wang, X., Ge, T., Xu, C., Xue, Y., Luo, C., 2016b. Carbon isotopic (14C and 13C) characterization of fossil-fuel derived dissolved organic carbon in wet precipitation in Shandong Province, China. J. Atmos. Chem. 73, 207–221.

Wang, Z.-J., et al., 2020. Rainfall driven nitrate transport in agricultural karst surface river system: Insight from high resolution hydrochemistry and nitrate isotopes. Agric. Ecosyst. Environ. 291, 106787.

Wei, J., et al., 2019a. Estimating 1-km-resolution PM2.5 concentrations across China using the space-time random forest approach. Remote Sens. Environ. 231, 111221.

Wei, J., et al., 2019b. Satellite-Derived 1-km-Resolution PM1 Concentrations from 2014 to 2018 across China. Environ. Sci. Technol. 53, 13265–13274.

Wei, J. *et al.*, Improved 1 km resolution PM2.5 estimates across China using enhanced space–time extremely randomized trees, Atmos. Chem. Phys. 20(2020), pp. 3273–3289.

Willey, J.D., Kieber, R.J., Eyman, M.S., Avery Jr., G.B., 2000. Rainwater dissolved organic carbon: Concentrations and global flux. Glob. Biogeochem. Cycles 14, 139–148.

Willey, J.D., Kieber, R.J., Avery, G.B., 2006. Changing Chemical Composition of Precipitation in Wilmington, North Carolina, U.S.a.: Implications for the Continental U.S.a. Environ. Sci. Technol. 40, 5675–5680.

Witkowska, A., Lewandowska, A.U., 2016. Water soluble organic carbon in aerosols (PM1, PM2.5, PM10) and various precipitation forms (rain, snow, mixed) over the southern Baltic Sea station. Sci. Total Environ. 573, 337–346.

Wu, Q., Han, G., Tao, F., Tang, Y., 2012. Chemical composition of rainwater in a karstic agricultural area, Southwest China: the impact of urbanization. Atmos. Res. 111, 71–78.

Xiao, H.W., Xiao, H.Y., Long, A.M., Wang, Y.L., Liu, C.Q., 2013. Chemical composition and source apportionment of rainwater at Guiyang, SW China. J. Atmos. Chem. 70, 269–281.

Xiao, H.-W., Xiao, H.-Y., Long, A.-m., Wang, Y.-L., 2012. Who controls the monthly variations of NH4+ nitrogen isotope composition in precipitation? Atmos. Environ. 54, 201–206.

Xing, J., et al., 2019. Atmospheric wet deposition of dissolved organic carbon to a typical anthropogenic-influenced semi-enclosed bay in the western Yellow Sea, China: Flux, sources and potential ecological environmental effects. Ecotoxicol. Environ. Saf. 182, 109371.

Yan, F., et al., 2019. Deposition of Organic and Black Carbon: Direct Measurements at three Remote Stations in the Himalayas and Tibetan Plateau. J. Geophys. Res.-Atmos. 124, 9702–9715.

Yan, G., Kim, G., 2012. Dissolved organic carbon in the precipitation of Seoul, Korea: Implications for global wet depositional flux of fossil-fuel derived organic carbon. Atmos. Environ. 59, 117–124.

Yue, F.J., Li, S.L., Liu, C.Q., Lang, Y.C., Ding, H., 2015. Sources and transport of nitrate constrained by the isotopic technique in a karst catchment: an example from Southwest China. Hydrol. Process. 29, 1883–1893.

Yue, F.-J., et al., 2019. Land use interacts with changes in catchment hydrology to generate chronic nitrate pollution in karst waters and strong seasonality in excess nitrate export. Sci. Total Environ. 696, 134062.

Zeng, J., et al., 2019. Quantifying depression trapping effect on rainwater chemical composition during the rainy season in karst agricultural area, southwestern China. Atmos. Environ. 218, 116998.

Zeng, J., Han, G., Wu, Q., Tang, Y., 2020a. Effects of agricultural alkaline substances on reducing the rainwater acidification: Insight from chemical compositions and calcium isotopes in a karst forests area. Agric. Ecosyst. Environ. 290, 106782.

Zeng, J., et al., 2020b. Agriculture driven nitrogen wet deposition in a karst catchment in

Southwest China. Agric. Ecosyst. Environ. 294, 106883.
Zeng, J., et al., 2020c. Determining rainwater chemistry to reveal alkaline rain trend in Southwest China: Evidence from a frequent-rainy karst area with extensive agricultural production. Environ. Pollut. 266, 115166.
Zhang, et al., 2008. Nitrogen inputs and isotopes in precipitation in the North China Plain. Atmos. Environ. 42, 1436–1448.
Zhang, Y., Lee, X., Cao, F., Huang, D., 2011. Seasonal variation and sources of low molecular weight organic acids in precipitation in the rural area of Anshun. Chin. Sci. Bull. 56, 1005–1010.
Zhang, Z., Chen, X., Soulsby, C., 2017. Catchment-scale conceptual modelling of water and solute transport in the dual flow system of the karst critical zone. Hydrol. Process. 31, 3421–3436.
Zhang, Z., et al., 2020. Coupled hydrological and biogeochemical modelling of nitrogen transport in the karst critical zone. Sci. Total Environ. 732, 138902.